with Smad4 (co-Smad) to translocate into the nucleus to directly or indirectly regulate the transcription of target genes (7, 8). BMPs and their receptors are expressed throughout the growth plate and perichondrium of developing bone (9). BMPs maintain expression of *Sox9* and subsequent cartilage matrix production (10, 11). BMPs are also required *in vitro* for the induction of *Col2a1* and *Col10a1* to promote chondrocyte maturation at later stages (12–14). Chondrocyte-specific overexpression of the extracellular BMP antagonist, Noggin, in transgenic mice resulted in no cartilage formation (15). Similarly, mice with cartilage-specific combined deletions of two BMP type I receptor genes (*Bmpr1a* and *Bmpr1b*), or with a double knock-out of *Smad1* and *Smad5*, showed severely impaired chondrogenesis (16, 17). At a later maturation stage, BMP signaling directly accelerates the expression of *Col10a1* in concert with Runx2 (13, 18, 19). Forced expression of constitutively active *Bmpr1a* in cartilage promoted the maturation and hypertrophy of chondrocytes in mice (20). The evidence clearly demonstrates the accelerating roles of BMP signaling in chondrocyte commitment, proliferation, and hypertrophic maturation both *in vivo* and *in vitro*.

Chondrogenesis in the endochondral ossification process is a promising cellular event for application in cartilage and bone regeneration, and it is a process that can be artificially engineered from human mesenchymal stem/stroma cells (MSCs) (21). Regarding the treatment of articular cartilage defects, the engineered chondrocytes must arrest maturation processes, because abnormally matured hypertrophic chondrocytes, expressing *COL10A1*, mineralize cartilage matrix to cause pathological conditions such as osteoarthritis (OA) (22–24). This is a major problem of cartilage tissue engineering in an *in vitro* culture system, where MSCs rapidly express *COL10A1* in a monolayer or pellet culture before the cells express hypertrophic phenotypes, suggesting that the mechanism by which MSCs induce type X collagen expression *in vitro* is different from that in chondrogenesis *in vivo* (25, 26). In bone engineering events, MSCs have formed bone trabeculae *in vivo* only when they had developed hypertrophic chondrocyte structure *in vitro* prior to implantation (21). Therefore, controlling the maturation and hypertrophy of chondrocytes is crucial for regenerative medicine of both cartilage and bone.

Although the effects of BMP signaling in promoting chondrocyte maturation should be eliminated for cartilage regeneration, they may be artificially enhanced to promote the efficiency of bone engineering. Although the BMP-Smad pathway directly induces the inhibitory Smad, Smad6, to inhibit the phosphorylation of Smad1/5/8 as a negative feedback mechanism (27), and Smurf1 targets Smad6 and the BMP type I receptors to block BMP signaling (28, 29), these inhibitory molecules are not specifically expressed in maturing chondrocytes. Recently, we reported that expression of the transcriptional repressor SnoN gradually increases in BMP-induced differentiating chondrocytes to suppress BMP signaling and the subsequent chondrocyte hypertrophic maturation (30). However, because SnoN partially blocked chondrocyte maturation, the mechanism regulating the rate of BMP signaling-driven chondrocyte differentiation in a cell-autonomous manner remains unclear.

The membrane-bound enzyme neutral sphingomyelinase 2 (nSMase2), encoded by the sphingomyelin phosphodiesterase 3 (*Smpd3*) gene, cleaves sphingomyelin to generate the lipid second messenger ceramide, which affects a variety of cellular process, including proliferation, apoptosis, and differentiation (31–34). A deletion mutation in the *Smpd3* gene was identified in fragilitas ossium (*fro*), a mouse model of osteogenesis imperfecta (35). *fro/fro* mice are characterized by retarded skeletal growth and a severely hypomineralized skeleton with normal osteoblast differentiation; bone mineralization can be rescued by osteoblast-specific overexpression of *Smpd3*, suggesting an important role of nSMase2 in the mineralization of the extracellular matrix (36). Interestingly, the number and area of hypertrophic chondrocytes were significantly increased, and conversion of cartilage into bone was retarded in *fro/fro* bone. *Smpd3* knock-out mice also showed fragile bones and dwarfism, with retarded transition of proliferative chondrocytes into hypertrophic chondrocytes (37, 38). Importantly, the knee joint cartilage of adult *Smpd3*-null mice showed severe deformity with exostosis, the phenotype of OA (38). These findings, from two lines of nSMase2 loss-of-function mice, suggest that *Smpd3*/nSMase2 plays an important role in suppressing hypertrophic maturation of chondrocytes and OA initiation. However, there is currently no information regarding the molecular mechanism for the function of nSMase2 in chondrocyte differentiation. In C2C12 myoblasts, BMP-2-induced Runx2 directly binds to the *Smpd3* promoter to up-regulate expression, suggesting that BMP signaling could elevate *Smpd3* level in a certain context (39).

In this study, we report that *Smpd3* is continuously up-regulated by BMP-2 stimulation of chondrocytes during the maturation stage to suppress the late differentiation step via the Akt pathway. We found that this induction of *Smpd3* by BMP-2 was Runx2-dependent and that the transcription factor is crucial for the hypertrophic maturation of chondrocytes. Loss- and gain-of-function experiments revealed that *Smpd3*/nSMase2 or ceramide signaling cell-autonomously suppressed expression of *Col2a1*, *Col10a1*, and hyaluronate synthase 2 (*Has2*), as well as accumulation of glycosaminoglycan. The Akt-S6 pathway was found to be responsible for the action of *Smpd3*/nSMase2. Importantly, application of an inhibitor compound for nSMase into the mouse bone organ culture system significantly increased the hypertrophic conversion and extracellular matrix calcification of cartilage.

EXPERIMENTAL PROCEDURES

Cell Culture and Differentiation—The mouse chondrogenic cell line ATDC5, established from a differentiated culture of the teratocarcinoma stem cell line AT805 on the basis of chondrogenic potential (40), was obtained from the RIKEN BioResource Center. Human chondrocyte cell line C28/I2 was a kind gift from Dr. Mary Goldring (41). The cells were cultured in Dulbecco's modified Eagle's medium (DMEM)/Ham's F-12 (1:1) (Invitrogen), containing 5% fetal bovine serum (FBS) with 100 units/ml penicillin G and 100 μg/ml streptomycin. The mouse C3H10T1/2 cell line was obtained from the ATCC. The cells were cultured in Eagle's basal medium (Sigma) with 2 mM L-glutamine, 10% FBS, 100 units/ml penicillin G, and 100 μg/ml

streptomycin. Primary chondrocytes were harvested from 2-day-old mice with a C57BL/6J background. Briefly, articular cartilage of the femoral heads, femoral condyles, and tibial plateaus was isolated from mice and digested by 3 mg/ml collagenase D (Roche Applied Science) for 45 min, followed by 0.5 mg/ml collagenase D overnight. The chondrocytes were filtered through a sterile 40-μm cell strainer and cultured in DMEM/Ham's F-12 (1:1) containing 10% FBS, 100 units/ml penicillin G, and 100 μg/ml streptomycin. Differentiation of the cells, cultured in monolayer, was induced by the addition of recombinant human BMP-2 (PeproTech) at a concentration of 300 ng/ml, with or without insulin/transferrin/selenium (ITS) supplement (Sigma) on collagen type I-coated culture plates (Iwaki).

Embryonic Bone Organ Culture—Metatarsal bone rudiments were harvested from C57BL/6J mouse embryos at 16.5 days post-coitum (E16.5) and cultured in DMEM/Ham's F-12 (1:1) supplemented with 10% FBS, and 100 units/ml penicillin G, and 100 μg/ml streptomycin, as described (42). Cultured bones were stained with Alcian blue and alizarin red dyes according to a standard protocol for skeletal preparation. Briefly, bones fixed in 96% ethanol were stained with 0.015% Alcian blue 8GX (Sigma) in a mixture solution of 96% ethanol/acetic acid (4:1) for 1 day, followed by a dehydration step in 100% ethanol. Dehydrated bones were immersed briefly in 1% potassium hydroxide (KOH), followed by staining in 0.001% alizarin red S (Sigma) in 1% KOH for 1 day. Images were captured with stereomicroscope M165FC (Leica). Four bones per group were analyzed. Animal experiments were approved by the Institutional Animal Care and Use Committee of Kagoshima University (number MD12043).

RNA Interference—Dharmacon siRNA ON-TARGETplus SMARTpool, a mixture of four independent siRNAs against mouse *Runx1*, *Runx2*, *Runx3*, *Smpd3*, or *Has2*, and the control reagent were purchased from Thermo Scientific. siRNAs were transfected into cells using Lipofectamine RNAiMax (Invitrogen). BMP-2 and compounds were added to the culture simultaneously after an overnight transfection of siRNA.

Plasmids and Adenovirus—Mouse *Smpd3* cDNA was cloned from ATDC5 by employing an RT-PCR-based technique, subcloned into the entry vector, pENTR, and further transferred into the C-terminally V5-tagged expression vector, pEF-DEST51, by attL-attR recombination (Invitrogen). To generate adenovirus-carrying *Smpd3* cDNA, the *Smpd3* gene in the pENTR-Smpd3 vector was transferred into the C-terminally V5-tagged adenovirus expression vector pAd/CMV/V5-DEST by attL-attR recombination (Invitrogen) and further transfected into the adenovirus-producing cell line 293A according to the manufacturer's protocol. pAd/CMV/V5-GW/lacZ adenovirus expression vector was used as a control to express β-galactosidase. Adenovirus infection into ATDC5 cells was performed at a multiplicity of infection of 10. These experiments were approved by the Kagoshima University safety control committee for gene recombination techniques (number 22053).

Chemical Inhibitor Compounds and C_2-ceramide—All of the following agents were resolved in dimethyl sulfoxide (DMSO), and DMSO was used as the mock control. Cycloheximide was purchased from Sigma and applied at a concentration of 10 mM for 2 h, prior to BMP-2 stimulation. The nSMase inhibitor, GW4869 (Sigma), or C_2-ceramide (Enzo Life Sciences) was applied at the same time of BMP-2 induction, at 1 or 10 μM, respectively. The PI3K inhibitor, LY294002 (Sigma), Akt inhibitor, MK2206 (Chemie Tek), and the mammalian target of rapamycin inhibitor (Sigma) were applied at the same time of BMP-2 induction, at the indicated concentrations.

Immunoblotting and RTK Signaling Antibody Array Analysis—Cells were lysed in M-PER lysis buffer (Thermo Scientific) supplemented with aprotinin, sodium orthovanadate, and phenylmethylsulfonyl fluoride (PMSF) and subjected to SDS-PAGE, membrane transfer, and chemiluminescence, using standard protocol. Blots were incubated with the following: anti-Runx2 (1:1,000, 8G5, MBL); anti-nSMase2 (1:500, H-195, Santa Cruz Biotechnology); anti-aggrecan (1:500, H-300, Santa Cruz Biotechnology); anti-collagen type II α1 (1:1,000, LSBio); anti-phospho-Akt (Ser-473) (1:1,000, 587F11, Cell Signaling); anti-Akt (1:1,000, 5G3, Cell Signaling); anti-phospho-S6 ribosomal protein (Ser-235/236) (1:1,000, D57.2.2E, Cell Signaling); anti-S6 ribosomal protein (1:1,000, 54D2, Cell Signaling); anti-phospho-PI3K (1:1,000, number 4228, Cell Signaling); anti-PI3K (p85) (1:1,000, number 610045, BD Transduction Laboratories); anti-phospho-Smad1/5/8 (1:1,000, number 9511, Cell Signaling); anti-Smad1 (1:1,000, number 9743, Cell Signaling); and horseradish peroxidase (HRP)-conjugated anti-rabbit secondary antibody, anti-mouse secondary antibody (1:10,000) (Cell Signaling), or anti-tubulin antibody (1:1,000, DM1A, T9026, Sigma). Signals were detected using the LAS 4000 Mini Image Analyzer (Fujifilm). We employed PathScan® RTK signaling antibody array kit (Cell Signaling) to analyze the signaling pathway influenced by loss of Smpd3/nSMase2 function. This system is a slide-based antibody array, founded upon the sandwich immunoassay principle and allowing for the simultaneous detection of 28 receptor tyrosine kinases and 11 important signaling nodes when phosphorylated at tyrosine or other residues, was employed to analyze the signaling pathway influenced by loss of *Smpd3*/nSMase2 function. The experiment was performed according to the manufacturer's manual, and the chemiluminescent readout was performed with LAS 4000 Mini Image Analyzer.

Immunocytochemistry and Immunohistochemistry—For immunocytochemistry, cells were fixed with 4% paraformaldehyde in PBS for 30 min and treated with 0.2% Triton X-100. CAS block (Zymed Laboratories Inc.) was used for blocking. For immunohistochemistry, formalin-fixed mouse E17.5 embryo humeri were embedded in paraffin blocks, which were sliced at a 4-μm thickness. The antigen was retrieved by the Liberate Antibody Binding solution (Polysciences). A CAS block was used for blocking. Cells or bone sections were incubated with anti-aggrecan (1:100, H-300, Santa Cruz Biotechnology), anti-collagen type II α1 (1:100, LSBio), anti-nSMase2 rabbit polyclonal antibody (1:100, H-195, Santa Cruz Biotechnology), and anti-Has2 mouse monoclonal antibody (1:100, D-8, Santa Cruz Biotechnology). Anti-mouse Alexa Fluor 488 (1:200, A11001) or anti-rabbit Alexa Fluor 568 (1:200, A11011) (Invitrogen) was used to detect signals. Normal rabbit or mouse IgG was used as negative control. Hyaluronan (HA) detection

involved the following protocol. Samples were blocked with a streptavidin/biotin blocking kit (Vector Laboratories), according to the manufacturer's protocol, and digested sequentially with 0.05% of trypsin and 1 unit/ml of chondroitinase ABC (Sigma). Samples were further blocked with CAS block and sequentially incubated with biotin-conjugated HA-binding protein (1:1,000, Hokudo) and 1 μg/ml Alexa Fluor 488-conjugated streptavidin (Invitrogen). Images of immunocytochemistry and immunohistochemistry were captured with microscope AX80 and digital camera DP70 (Olympus). Animal experiments were approved by the Institutional Animal Care and Use Committee of Kagoshima University (number MD12043).

Real Time Quantitative PCR Assay—Cells were lysed with the TRIzol reagent (Invitrogen) to purify RNA, and 1 μg of RNA was reverse-transcribed into cDNA using the Verso cDNA kit (Thermo Scientific). The relative amount of gene transcripts was determined by real time PCR using the SYBR premix Ex TaqII (Takara) and the Thermal Cycler Dice TP850 (Takara). PCRs were performed in duplicate per sample, and the measured expression level of each gene was normalized to that of *Hprt1*. ΔC_t values were calculated by subtracting C_t values of *Hprt1* from C_t values of target genes. Sequence information of primers used is listed in supplemental Table 1.

TUNEL Assay—For detecting ATDC5 cells that underwent apoptosis, we used the ApopTag® peroxidase *in situ* apoptosis detection kit (Merck), which detects apoptotic cells *in situ* by labeling and detecting DNA strand breaks by the TUNEL method. The apoptotic cells were visualized by immunoperoxidase staining. Four independent experiments were performed, and four fields per well were evaluated for the number of apoptotic cells.

Statistical Analysis—Data in this study are expressed as mean ± S.D. of three independent experiments, unless otherwise noted. The statistical comparisons between the different treatments were performed using an unpaired Student's *t* test in which $p < 0.05$ was considered significant and $p < 0.01$ was highly significant.

RESULTS

Smpd3 Is Induced by BMP-2 in Chondrocytes and Is Detected in Mature Chondrocytes in Vivo—We hypothesized that BMP signaling cell-autonomously activated unknown mechanisms to terminate BMP-induced chondrocyte differentiation through a negative feedback pathway. We focused on the *Smpd3* gene, because it could be up-regulated by BMP-2 in C2C12 myoblasts of mesenchymal origin (39); loss-of-function models for *Smpd3* in mice showed an increased number of hypertrophic chondrocytes or retarded transition of proliferative chondrocytes into hypertrophic chondrocytes. Molecular mechanisms for both cartilage phenotypes are unclear (37, 38), suggesting a relationship between BMP signaling and *Smpd3*/nSMase2 in chondrogenesis. To investigate the possible cell-autonomous roles of *Smpd3* in chondrocyte maturation, we mainly employed the clonal chondrogenic mouse cell line ATDC5 because it is an excellent *in vitro* model for skeletal development, which can be stimulated by BMP-2 (43, 44). We also used the normal human chondrocyte cell line C28/I2, mouse chondrogenic cell line C3H10T1/2, and mouse primary articular chondrocytes. We used BMP-2 to stimulate chondrogenic differentiation because, in addition to existing evidence, we and others have observed strong expression of the BMP-2 protein in proliferating and mature chondrocytes in the developing bones of rodents (45, 46). We first checked if these cell lines could differentiate into chondrocytes and mature into hypertrophic chondrocytes and not fibrochondrocytes. Upon BMP-2 induction, ATDC5 cells could produce chondrocyte-specific proteins, aggrecan and type II collagen, in the extracellular matrix (Fig. 1*A*). The early chondrocyte differentiation marker aggrecan (*Acan*) was elevated after day 1 and was maintained at elevated levels for 2 weeks, whereas *Col10a1* increased mildly from day 3 and was strongly up-regulated after day 7. *Col1a1* and *Col3a1* gene expression was not elevated, but rather decreased, suggesting that these cells did not differentiated into fibrochondrocytes (Fig. 1*B*). Similar results were obtained in C28/I2 cells (Fig. 1, *C* and *D*) and C3H10T1/2 cells (Fig. 1*E*). We also confirmed chondrogenic differentiation of primary chondrocytes by BMP-2 (Fig. 1*F*). ΔC_t values of quantitative PCR data indicated that primary chondrocytes express higher levels of chondrocyte marker genes than the three chondrogenic cell lines, suggesting that primary chondrocytes are already committed and differentiated into chondrocytes without BMP-2 induction, whereas the cell lines are relatively immature to differentiate into chondrocytes upon BMP stimulation. From these expression profiles, we considered these cell lines to be suitable models for chondrocyte differentiation. In ATDC5 cells, *Smpd3* showed a varied expression pattern from that of *Acan* and *Col10a1*, in that it was strongly elevated from day 1 and showed a second peak of increase after day 7 (Fig. 1*G*). We also observed the BMP-2-induced increment of the *Smpd3* gene in C28/I2, C3H10T1/2, and primary chondrocytes (Fig. 1*H*). Importantly, the primary chondrocytes also expressed higher levels of *Smpd3*, suggesting its functional importance in chondrocytes. If *Smpd3*/nSMase2 has an *in vivo* role in chondrogenesis or cartilage maintenance, it would be expressed in cartilage, although its expression in cartilage has not been characterized in detail. Quantitative PCR analysis on a panel of cDNAs from multiple tissues generated from 3-month-old mice revealed that *Smpd3* was expressed at the highest levels in the thymus, intestine, skin, fat, and bone, although it was almost absent in the heart, liver, and kidney (Fig. 1*I*). *Smpd3* was moderately expressed in cartilage tissue. This expression profile of *Smpd3* is essentially similar to the results reported for 2-week-old mice (36). In embryonic bone, we detected prominent expression of *Smpd3*-coding nSMase2 protein in the bone collar and trabecular bone by immunofluorescence (Fig. 1*J*). In the cartilage, little nSMase2 expression was noted in resting and columnar proliferating chondrocytes, whereas relatively high expression was observed in the prehypertrophic layer and hypertrophic chondrocytes (Fig. 1*J*), with an expression pattern resembling that of Runx2 (4).

BMP-2-induced Increase of Smpd3 Expression Is Runx2-dependent—We wondered if this BMP-2-induced expression of *Smpd3* in ATDC5 was directed by the BMP-Smad signaling axis, although the expression pattern was not the typical rapid pattern of a gene that is directly targeted (47). To test this, we treated ATDC5 cells with cycloheximide (CHX), an inhibitor of

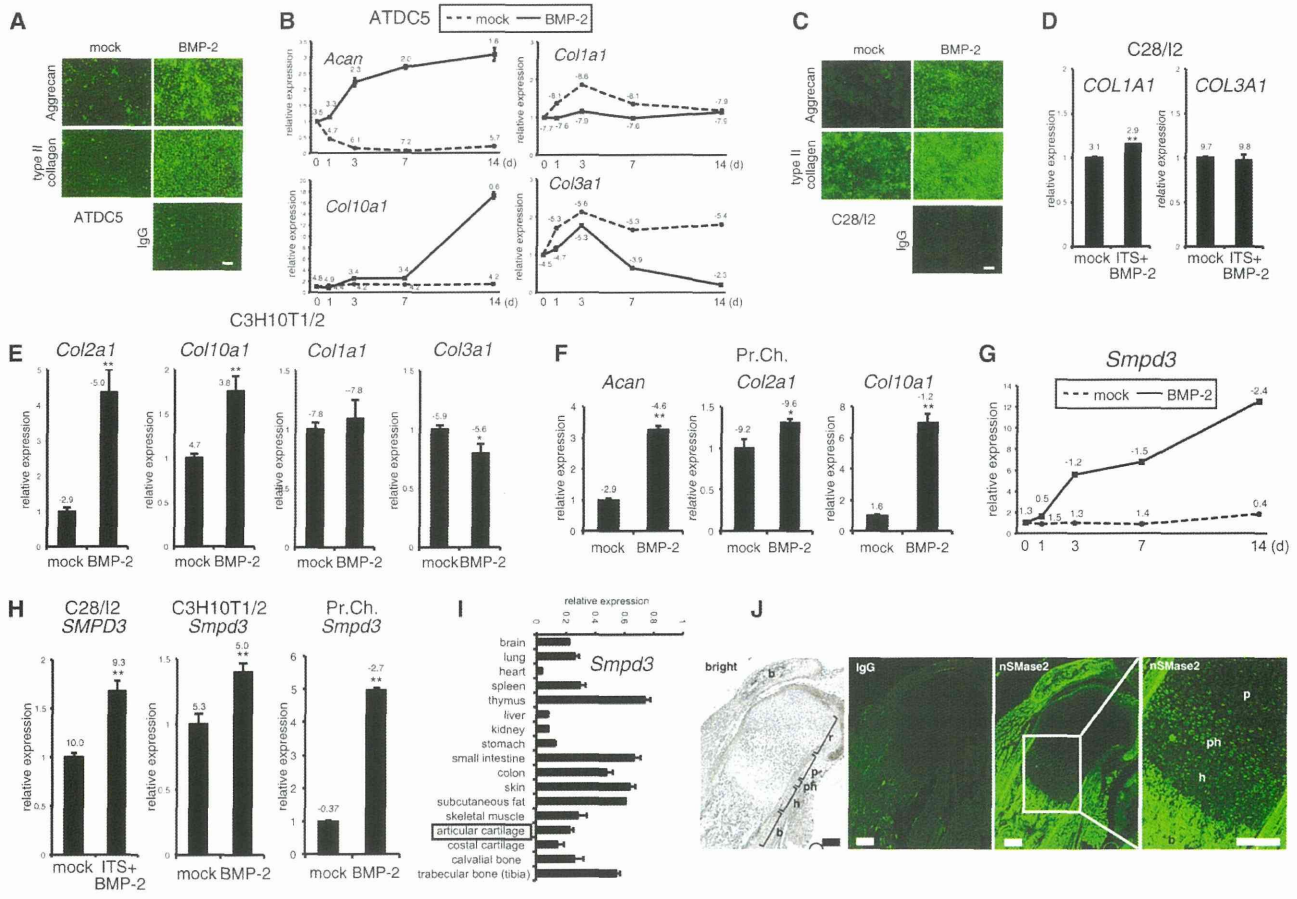

FIGURE 1. **Expression of *Smpd3*/nSMase2 is promoted by BMP-2 treatment in maturing chondrocytes *in vitro* and is increased in prehypertrophic and hypertrophic chondrocytes in a growth plate *in vivo*.** *A*, chondrogenic differentiation of mouse ATDC5 chondrocytes was induced by application of BMP-2 (300 ng/ml) for 7 days (*d*). Immunofluorescence for aggrecan or type II collagen was performed, with normal IgG as negative control. *Scale bar*, 100 μm. *B*, ATDC5 cells were cultured in the presence of BMP-2 (300 ng/ml) for the indicated periods. Expression levels of *Acan*, *Col10a1*, *Col1a1*, and *Col3a1* were examined by quantitative RT-PCR. *C*, chondrogenic differentiation of human C28/I2 chondrocytes was induced by the application of BMP-2 (300 ng/ml) for 7 days. Immunocytochemistry for aggrecan or type II collagen was performed, with normal IgG as negative control. *Scale bar*, 100 μm. *D*, C28/I2 chondrocytes were cultured in presence of BMP-2 (300 ng/ml) and ITS supplement for 14 days. Expression of *COL1A1* or *COL3A1* was evaluated by quantitative RT-PCR. *E*, mouse C3H10T1/2 cells were cultured with BMP-2 (300 ng/ml) for 48 h. Expression levels of *Col2a1*, *Col10a1*, *Col1a1*, and *Col3a1* were evaluated by quantitative RT-PCR. *F*, mouse primary chondrocytes (*Pr.Ch.*) cells were cultured in the presence of BMP-2 (300 ng/ml) for 6 days. Expression levels of *Acan*, *Col2a1*, and *Col10a1* were evaluated by quantitative RT-PCR. *G*, ATDC5 cells were cultured in presence of BMP-2 (300 ng/ml) for the indicated periods. Expression of *Smpd3* was examined by quantitative RT-PCR. *H*, quantitative RT-PCR for *Smpd3* was performed on samples in *D*, *E*, and *F*. *I*, real time PCR for *Smpd3* was performed on a tissue cDNA panel of a 3-month-old mouse. *J*, expression of nSMase2 in mouse E17.5 humerus cartilage was evaluated by immunofluorescence. Normal IgG was used as negative control. *r*, resting chondrocytes; *p*, proliferating chondrocytes; *ph*, prehypertrophic chondrocytes; *h*, hypertrophic chondrocytes; *b*, bone. *Scale bar*, 200 μm. *, $p < 0.05$; **, $p < 0.01$. ΔC_t values (C_t target − C_t Hprt1) of quantitative RT-PCR are indicated in the *graphs*.

de novo protein synthesis, before adding BMP-2. As expected, 24 h after BMP-2 stimulation, the induction of *Id1*, a representative direct-target gene of the BMP-Smad pathway, was maintained, even in the presence of CHX (Fig. 2*A*). Induction of *Id1* was higher in CHX-treated cells, likely because of the suppression of inhibitory Smad6 synthesis (27). However, expression of *Col2a1* was eliminated by CHX treatment (Fig. 1*A*). This basal suppression by CHX probably results from an inhibition of the constitutive expression of Sox9 and downstream Sox5 and Sox6, transcription factors that cooperatively activate the promoter of *Col2a1* (2, 48). However, existing Sox proteins should be responsible for the partially increased expression of *Col2a1* by BMP-2. The basal expression level of *Smpd3* was also suppressed by CHX treatment. Unlike *Col2a1*, however, the CHX-eliminated basal expression of *Smpd3* was not up-regulated by BMP-2 (Fig. 2*A*) suggesting that a *de novo* protein other than the Sox trio was necessary for BMP-induced expression of *Smpd3* in ATDC5 cells. Because the Runx2 protein is a master regulator of chondrocyte maturation (4, 5), and its direct interaction with the *Smpd3* promoter is important for its expression in myoblasts (39), we investigated the relationship between Runx2 and expression of *Smpd3* in chondrocytes. We confirmed the increment of the *Runx2* gene during BMP-induced maturation of ATDC5 chondrocytes (Fig. 2*B*). To address this question, we transfected ATDC5 cells with *Runx2* siRNA. At day 2 of BMP-2 application, *Runx2* was weakly induced, and its expression was knocked down by the siRNA to about 40% that of the control (Fig. 2*C*). Expression of *Id1* was not decreased by siRunx2, but rather it was increased, suggesting that Runx2 is inhibitory of the BMP pathway during this early differentiation stage. Interestingly, loss of Runx2 not only suppressed basal expression of *Smpd3* but also completely blocked induction by

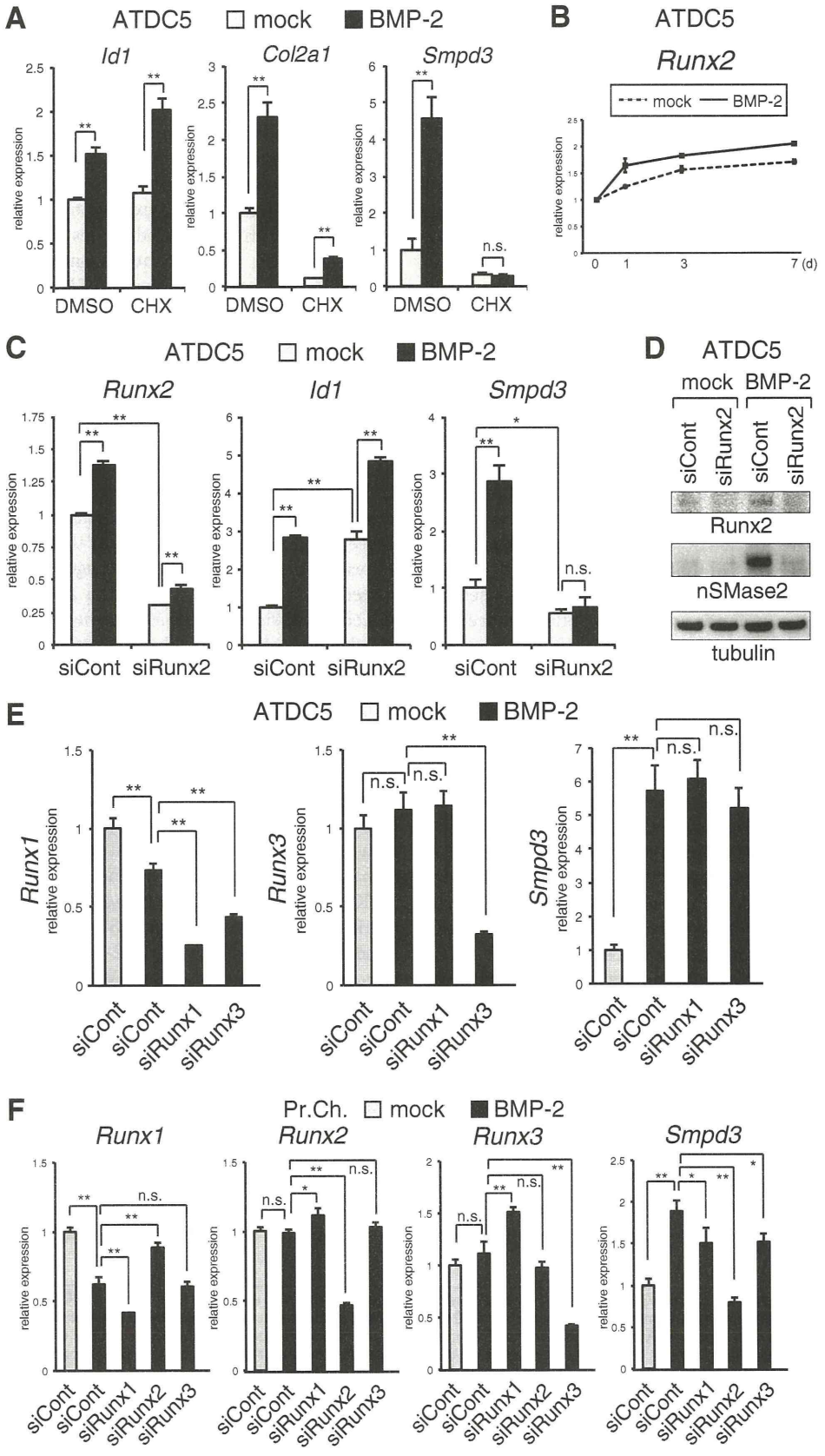

BMP-2 treatment (Fig. 2*C*). This effect of siRunx2 was confirmed by analyzing protein expression of nSMase2 using immunoblotting (Fig. 2*D*). To assess the functional specificity of Runx2 among the three Runx isoforms, siRNAs for *Runx1* and *Runx3* were tested in ATDC5 cells. Although we could obtain efficient knockdown of *Runx1* and *Runx3*, the BMP-2-induced increase of *Smpd3* was not blocked by the corresponding siRNA (Fig. 2*E*). In primary chondrocytes, knockdown of *Runx2* completely abrogated the BMP-stimulated up-regulation of *Smpd3* (Fig. 2*F*). In contrast to ATDC5 cells, silencing of *Runx1* or *Runx3* could mildly suppress expression of *Smpd3* in primary chondrocytes (Fig. 2*F*), suggesting that Runx1 and Runx3 were partially responsible for *Smpd3* expression. These data demonstrate that BMP signaling increases the expression of *Smpd3*/nSMase2 in chondrocytes in cooperation with Runx2, especially in the maturation stages when the level of *Runx2* is elevated.

Smpd3/nSMase2 and C_2-ceramide Inhibit Chondrogenic Differentiation and Maturation of Chondrocytes—We used a knockdown assay to investigate whether *Smpd3*/nSMase2 has a role in the differentiation of ATDC5 chondrocytes. The potent induction of *Smpd3* by BMP treatment was silenced by siSmpd3 at a level of ~25% of that in cells treated with control siRNA at day 6 (Fig. 3*A*). Loss of *Smpd3* mildly increased the basal level of *Col2a1* expression and significantly enhanced the BMP-2-induced increment (Fig. 3*A*). Although expression of *Col10a1* was not significantly elevated by BMP-2 at day 6, it was dramatically increased by siSmpd3 in the presence of BMP-2. Similar effects of siSmpd3 on the expression of *Col2a1* and *Col10a1* were observed in primary chondrocytes (Fig. 5*F*). This effect of *Smpd3* knockdown against expression of *Col2a1* was mimicked by the addition of 1 μM GW4869, a specific inhibitor compound for nSMase (Fig. 3*B*) (49), suggesting that the data from the siSmpd3 experiment resulted from down-regulation of nSMase2. GW4869 also enhanced the production of the cartilage-specific extracellular component, glycosaminoglycan, by BMP-2 stimulation for 17 days, as assessed by Alcian blue staining, both in ATDC5 cells and in primary chondrocytes (Fig. 3*C*). Because nSMase2 generates ceramide as a lipid second messenger from the cell membrane, and the total level of ceramide was decreased in *fro/fro* bone (36), we challenged the cell membrane-permeable C_2-ceramide to mimic nSMase-ceramide signaling. Combined application of GW4869 and C_2-ceramide completely eliminated the GW4869-mediated enhancement observed by Alcian blue staining (Fig. 3*C*). The effect of GW4869 or C_2-ceramide on Alcian blue staining was confirmed by immunoblotting for aggrecan (Fig. 3*C*). Although C_2-ceramide showed no effect on BMP-2-induced expression of *Smpd3* at day 14, it significantly suppressed the expression of both *Col2a1* and *Col10a1* (Fig. 3*D*). As another gain-of-function approach, adenovirus-mediated overexpression of *Smpd3* in ATDC5 cells was performed to yield transgene expression levels that were ~100 times those of endogenous levels even after 8 days of induction (Fig. 3*E*). Infection of *Smpd3*-expressing adenovirus presented similar results as those of the C_2-ceramide experiment, in which overexpression inhibited the BMP-2-mediated elevation of both *Col2a1* and *Col10a1* expression (Fig. 3*E*). Similarly, Smpd3-expressing adenovirus suppressed maturation of primary chondrocytes (Fig. 3*F*). These loss- or gain-of-function experiments suggest a cell-autonomous inhibitory action of the *Smpd3*/nSMase2-ceramide axis on maturation of chondrocytes.

Smpd3 Suppresses the Activity of the Akt-S6 Pathway during Chondrogenesis in Vitro—We sought the molecular mechanism by which Smpd3/nSMase2 suppresses chondrogenesis and focused on the Akt signaling pathway for the following reasons. First, phosphorylation of Akt and the downstream ribosomal protein S6 (rpS6) was increased in *fro/fro* fibroblasts (50). Second, genetic approaches revealed that the IGF-IGF receptor-PI3K-Akt pathway plays key roles in skeletal growth and endochondral ossification and that overexpression of the activated form of Akt in the cartilage of transgenic mice promoted chondrocyte differentiation and maturation, whereas forced expression of its dominant-negative form delayed these cellular events (51). To evaluate the specificity of Akt among the various RTK signaling pathways, we examined the possible correlation of the Akt pathway in *Smpd3*/nSMase2 signaling during chondrocyte differentiation by performing an RTK signaling antibody array assay. Because receptors for insulin or insulin-like growth factor (IGF), which promote chondrogenic differentiation of ATDC5 cells (40), are RTKs, and a mixture of ITS is preferentially used to prepare the chondrogenic condition of ATDC5 cells (52), we first checked the effect of application of the ITS supplement alone and found no effect on the RTK array (Fig. 4*A*). Interestingly, 8 h after the addition of BMP-2, phosphorylation of rpS6 was significantly strengthened. More importantly, BMP-2-enhanced rpS6 phosphorylation was further increased by GW4869 or *Smpd3* knockdown, and these loss-of-function conditions for *Smpd3*/nSMase2 induced mild phosphorylation of Akt (Fig. 4*A*), suggesting that Akt and rpS6 are the specific targets of inhibition. This notion was further supported by an immunoblot assay using ATDC5 cells treated with siSmpd3 or Smpd3-expressing adenovirus. Application of BMP-2, in combination with the ITS supplement, dramatically induced expression of the nSMase2 protein, which was clearly diminished by transfecting with siRNA for *Smpd3* (Fig. 4*B*), even after 20 h of stimulation. Phosphorylation of Akt, as well as of rpS6, was significantly increased by

FIGURE 2. **BMP-2-induced increase of *Smpd3* expression in chondrocytes is Runx2-dependent.** *A*, CHX was applied to ATDC5 cells at a concentration of 10 mM for 2 h prior to BMP-2 (300 ng/ml) stimulation. Cells were harvested 24 h after BMP-2 induction to perform quantitative RT-PCR analysis for *Id1*, *Col2a1*, and *Smpd3*. *B*, ATDC5 cells were cultured with BMP-2 (300 ng/ml) for the indicated times. Expression of *Runx2* was examined by quantitative RT-PCR. *C*, ATDC5 chondrocytes were transfected with control siRNA (*siCont*) or *Runx2* siRNA (*siRunx2*) for 16 h and then treated with or without BMP-2 (300 ng/ml) for 48 h. Quantitative RT-PCR analysis was performed for *Runx2*, *Id1*, and *Smpd3*. *D*, ATDC5 cells were transfected with control siRNA (*siCont*) or *Runx2* siRNA (*siRunx2*) for 16 h and stimulated with BMP-2 (300 ng/ml) for 48 h. Cells were subjected to immunoblot analysis for the indicated antibodies. Tubulin served as a loading control. *E*, ATDC5 cells were transfected with control siRNA (*siCont*), *Runx1* siRNA (*siRunx1*), or *Runx3* siRNA (*siRunx3*) for 16 h and then treated with or without BMP-2 (300 ng/ml) for 48 h. Quantitative RT-PCR analysis was performed for *Runx1*, *Runx3*, and *Smpd3*. *F*, mouse primary chondrocytes were transfected with control siRNA (*siCont*), *Runx1* siRNA (*siRunx1*), *Runx2* siRNA (*siRunx2*), or *Runx3* siRNA (*siRunx3*) for 16 h and then treated with or without BMP-2 (300 ng/ml) for 48 h. Quantitative RT-PCR analysis was performed for *Runx1*, *Runx2*, *Runx3*, and *Smpd3*. *, $p < 0.05$; **, $p < 0.01$; *n.s.*, not significant.

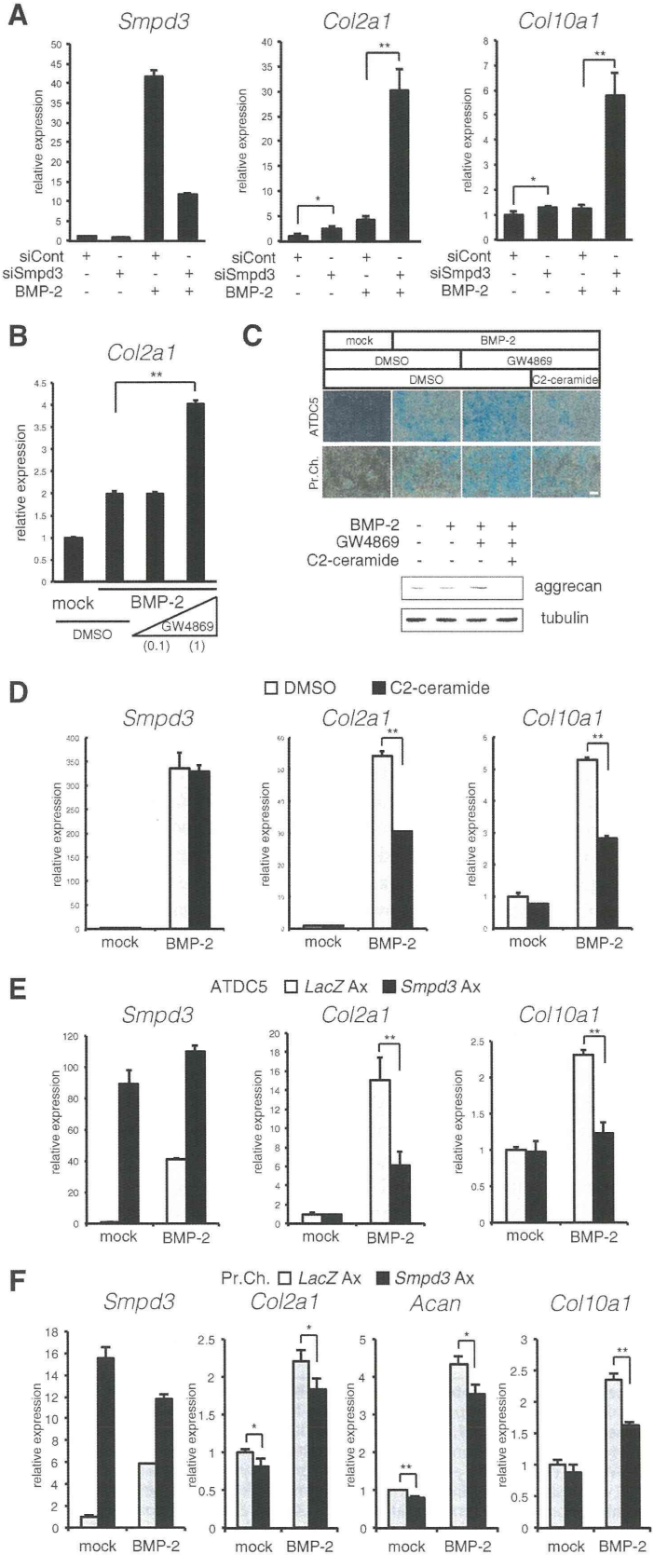

BMP-2 stimulation, although these proteins became more phosphorylated by the loss of *Smpd3* (Fig. 4*B*). Importantly, siSmpd3 increased the weak basal phosphorylation of both Akt and rpS6 in mock control cells, suggesting that neither ITS nor BMP-2 is crucial for the function of nSMase2. Overexpression of *Smpd3* weakened the induced phosphorylation of both Akt and rpS6 (Fig. 4*C*), whereas similar effects of Smpd3 adenovirus were observed in primary chondrocytes (Fig. 4*D*). Increased phosphorylation of Akt and rpS6 by the loss of *Smpd3* was also observed in primary chondrocytes (Fig. 4*D*) and C3H10T1/2 (Fig. 4*E*). The phosphorylation level of Smad1/5/8 was not altered by *Smpd3* knockdown (Fig. 4*E*), suggesting that the accelerated chondrogenic differentiation by siSmpd3 (Fig. 3*A*) was not due to an enhancement of BMP signaling. These results demonstrate an inhibitory function of *Smpd3*/nSMase2 against activation of Akt and rpS6 and a positive effect of BMP-2 in chondrocytes.

Smpd3 Suppresses Maturation of ATDC5 Chondrocytes via the PI3K-Akt Pathway—We next investigated the role of the Akt pathway in nSMase2-mediated inhibition of chondrogenesis in ATDC5 cells by employing specific inhibitor compounds. MK2206, an inhibitor for Akt, was tested for its ability to negate the enhanced chondrogenesis caused by loss of *Smpd3*. Expression of *Smpd3* in siSmpd3-treated cells was not further altered by MK2206 at concentrations between 1 and 3 μM, although 10 μM of the MK compound suppressed it (Fig. 5*A*). At day 6 of BMP-2 induction, MK2206 successfully suppressed the *Smpd3* siRNA-mediated increase of *Acan*, *Col2a1*, and *Col10a1*, in a dose-dependent fashion, at concentrations between 1 and 10 μM (Fig. 5*A*). Alcian blue staining revealed that the BMP-2-induced production of glycosaminoglycan, which was further stimulated by siSmpd3, was eliminated by the addition of MK2206 at 10 μM (Fig. 5*B*). We also investigated the participation of mammalian target of rapamycin, a downstream effector of Akt, by using its specific inhibitor, rapamycin. Although rapamycin suppressed the expression of *Smpd3*, it could block the siSmpd3-mediated up-regulation of *Col10a1* at 1 μM (Fig. 5*C*). Because total protein expression of PI3K, the upstream mediator of Akt, was significantly increased in *fro/fro* fibroblasts, which resulted in an up-regulated phosphorylation level of PI3K, we evaluated these in ATDC5 chondrocytes by an immunoblot assay. Indeed, phosphorylated, as well as total, PI3K protein was increased upon transfection with *Smpd3* siRNA (Fig. 5*D*). Therefore, a specific inhibitor for PI3K, LY294002, was tested with siSmpd3. LY294002 did not change the expression of *Smpd3* at concentrations between 1 and 5 μM, but a 25 μM concentration led to suppression. However, LY294002 did suppress the elevated expression of *Acan*, *Col2a1*, and *Col10a1* caused by the loss of *Smpd3*, in a dose-dependent manner at concentrations between 1 and 25 μM (Fig. 5*E*). The role of the Akt pathway was confirmed in primary chondrocytes by applying LY294002 (25 μM), MK2206 (5 μM), and rapamycin (0.5 μM); only MK2206 suppressed *Smpd3* expression (Fig. 5*F*). Hence, none of these inhibitor compounds increased expression of *Smpd3*, indicating that the inhibitory action on chondrocyte maturation was independent of *Smpd3* expression level. These data suggest that Smpd3/nSMase2 suppresses chondrocyte maturation, at least in part, via the PI3K-Akt pathway.

GW4869 or C_2-ceramide Promotes or Eliminates, Respectively, Terminal Hypertrophic Maturation of Chondrocytes in Mouse Bone Organ Culture—To further examine the role of the nSMase-ceramide signaling axis in relatively physiological conditions, we employed an *ex vivo* organ culture system of mouse embryonic metatarsal bone, a widely used method that permits the study of a complex chondrogenic process in a three-dimensional structure, in the context of native cell-cell and cell-extracellular matrix interactions and cellular signaling (42). The cartilage matrix was stained by Alcian blue, and the extracellular matrix calcified by mature hypertrophic chondrocytes was stained by alizarin red. The clear zone represents layers of uncalcified hypertrophic chondrocytes (Fig. 6*A*). All zone lengths were measured after image capturing (Fig. 6*B*). Blocking the function of nSMase by GW4869 solely enlarged both the clear zone and the calcified zone in a mild but statistically significant manner, a result similar to that seen by treatment with BMP-2 alone (Fig. 6, *A* and *B*, *2nd* and *3rd lanes*). Combined treatment with GW4869 and BMP-2 showed an additive effect (Fig. 6, *A* and *B*, *4th lane*), whereas C_2-ceramide eliminated the BMP-2-induced increase of the hypertrophic zone and, especially, the terminally differentiated calcified zone (Fig. 6, *A* and *B*, *5th lane*). Hence, GW4869 and C_2-ceramide exhibited opposite actions against BMP-2-driven acceleration in the hypertrophic conversion and terminal maturation of chondrocytes. In addition, C_2-ceramide clearly cancelled the additive promotion induced by GW4869 and BMP-2 (Fig. 6, *A* and *B*, *6th lane*). These results indirectly demonstrate the physiologically suppressive role of the nSMase2-ceramide pathway on chondrocyte maturation in cartilage/bone rudiments. Moreover, these data suggest a new strategy to control the rate of hypertrophic maturation in cartilage and bone regenerative medicine.

Apoptosis of terminally matured hypertrophic chondrocytes was reduced in the bone of *fro/fro* mice, a phenotype that accounted for the delayed onset of bone formation (36), suggesting an accelerating role for *Smpd3*/nSMase2 in the apoptosis of chondrocytes. To investigate whether this is a cell-autonomous event, we knocked down *Smpd3* in ATDC5 chondrocytes and performed a TUNEL assay to evaluate the

FIGURE 3. **Loss or gain of *Smpd3*/nSMase2 function promotes or suppresses BMP-2-induced chondrogenic maturation, respectively.** *A*, ATDC5 chondrocytes were transfected with control siRNA (*siCont*) or *Smpd3* siRNA (*siSmpd3*) for 16 h and then treated with or without BMP-2 (300 ng/ml) for 6 days. Quantitative RT-PCR analysis was performed for *Smpd3*, *Col2a1*, and *Col10a1*. *B*, ATDC5 cells were treated with BMP-2 (300 ng/ml) in combination with GW4869 at a concentration of 0.1 or 1 μM for 4 days to analyze expression of *Col2a1* by quantitative RT-PCR. *C*, ATDC5 cells or primary chondrocytes were stimulated with BMP-2 (300 ng/ml) in combination with GW4869 (1 μM) and C_2-ceramide (10 μM) for 17 days. Cells were subjected to Alcian blue staining. *Scale bar*, 200 μm. A parallel experiment was done with ATDC5 with a stimulation time of 7 days, and immunoblotting was performed for aggrecan and tubulin. *D*, ATDC5 cells were stimulated with BMP-2 (300 ng/ml) in combination with C_2-ceramide at 10 μM for 14 days. *E*, ATDC5 chondrocytes were infected with adenovirus (*Ax*) carrying *LacZ* or *Smpd3* for 2 h, and further cultured with or without BMP-2 (300 ng/ml) for 7 days. Expression of *Smpd3*, *Col2a1*, and *Col10a1* was evaluated by quantitative RT-PCR. *F*, mouse primary chondrocytes were infected with adenovirus carrying *lacZ* or *Smpd3* for 2 h and further cultured with or without BMP-2 (300 ng/ml) for 6 days. Expression of *Smpd3*, *Col2a1*, and *Col10a1* was evaluated by quantitative RT-PCR. *, $p < 0.05$; **, $p < 0.01$.

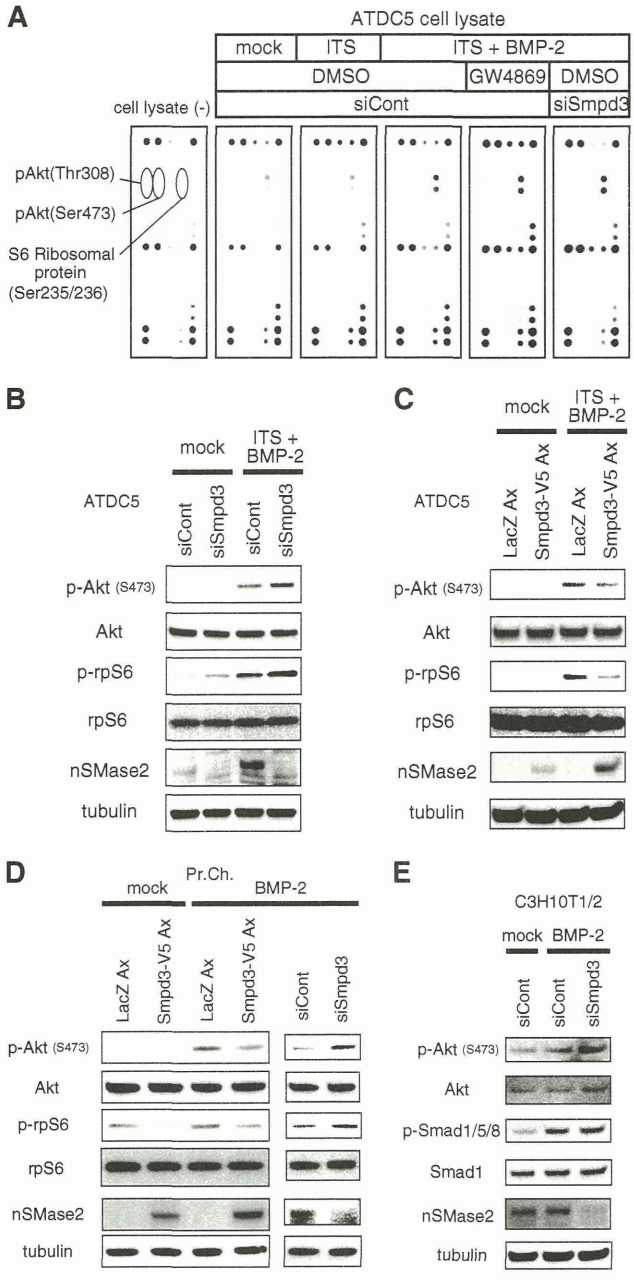

FIGURE 4. **Akt pathway is activated or repressed by loss or gain of *Smpd3* function, respectively.** *A*, ATDC5 cells were transfected with control siRNA (*siCont*) or *Smpd3* siRNA (*siSmpd3*) for 16 h, and then stimulated by a combination of ITS supplement and BMP-2 (300 ng/ml), with or without GW4869 (1 μM), for 8 h. Cells were analyzed by a PathScan® RTK signaling antibody array. *B* and *C*, ATDC5 cells were transfected with control siRNA (*siCont*) or *Smpd3* siRNA (*siSmpd3*) for 16 h (*B*) or infected with adenovirus (*Ax*) carrying *lacZ* or *Smpd3* for 2 h (*C*), and stimulated with the combination of ITS supplement and BMP-2 (300 ng/ml) for 20 h. Cells were subjected to immunoblot analysis for the indicated antibodies. Tubulin served as a loading control. *D*, mouse primary chondrocytes were infected with adenovirus carrying *lacZ* or *Smpd3* for 2 h or transfected with control siRNA (*siCont*) or *Smpd3* siRNA (*siSmpd3*) for 16 h and stimulated with BMP-2 (300 ng/ml) for 8 h. Cells were subjected to immunoblot analysis for the indicated antibodies. Tubulin served as a loading control. *E*, C3H10T1/2 cells were transfected with control siRNA (*siCont*) or *Smpd3* siRNA (siSmpd3) for 8 h and stimulated with BMP-2 (300 ng/ml) for 16 h. Cells were subjected to immunoblot analysis for the indicated antibodies. Tubulin served as a loading control.

effect on apoptosis (Fig. 6*C*). TUNEL-positive cells were counted after image capturing (Fig. 6*D*). Matured ATDC5 chondrocytes, stimulated by BMP-2 with ITS supplement for 6 days, showed hypertrophic morphology, and a substantial number of cells underwent apoptosis (Fig. 6, *C* and *D*). Indeed, transfection of *Smpd3* siRNA into maturing ATDC5 cells resulted in a statistically significant reduction in apoptosis (Fig. 6, *C* and *D*), suggesting that nSMase2 cell-autonomously accelerates apoptosis of hypertrophic chondrocytes.

Smpd3/nSMase2 Suppresses Expression of Has2 during Chondrogenesis via the PI3K-Akt Axis—Chondrocyte maturation is supported by hyaluronan, and embryonic limb mesoderm-specific ablation of hyaluronan synthase 2 (*Has2*) in mice resulted in reduced formation of zones for prehypertrophic and hypertrophic chondrocytes (53), suggesting a major role of Has2 in the three Has isoforms involved in the production of hyaluronan in cartilage. Recent studies have reported a significant level of *Has2* expression and hyaluronan synthesis in *fro/fro* fibroblasts and that nSMase2 suppressed production of Has2 via inactivation of Akt (50). Taken together, if *Smpd3*/nSMase2 also regulates expression of *Has2* in chondrocytes, Has2 might be another target for the inhibitory action of *Smpd3*/nSMase2 on chondrocyte hypertrophic maturation. We confirmed the crucial role of Has2 in chondrocyte differentiation and maturation; siRNA-mediated knockdown of *Has2* resulted in a decline in expression of *Col2a1* and *Col10a1*, both in ATDC5 cells (Fig. 7*A*) and primary chondrocytes (Fig. 7*B*). In ATDC5 chondrocytes, upon BMP-2 stimulation the expression of *Has2* was down-regulated by half at day 6, whereas silencing of *Smpd3* recovered the decline (Fig. 7*C*). Although expression of *Has1* and *Has3* was also suppressed by BMP-2 induction, *Smpd3* siRNA did not rescue the decrease (Fig. 7*C*), suggesting that only Has2, among the three Has isoforms, is a specific target of Smpd3 signaling in chondrocytes. This finding was confirmed using immunofluorescence for protein expression levels in ATDC5 cells (Fig. 7*D*) and primary chondrocytes (Fig. 7*E*), which indicated that although nSMase2 accumulated due to BMP-2 induction, the signals of Has2 protein were diminished. The merged images show the mutually exclusive expression of nSMase2 and Has2. Importantly, *Smpd3* knockdown rescued the weakened expression of Has2 protein (Fig. 7, *D* and *E*). The expression level of Has2 protein was reflected to the production of hyaluronan in primary chondrocytes (Fig. 7*E*). *In vivo*, both nSMase2 and Has2 were strongly expressed and co-localized in bone (Fig. 7*F*). In cartilage, however, Has2 was widely expressed in proliferating and resting chondrocytes with moderate strength, although it was diminished in the hypertrophic zone, where the expression pattern contrasted with that of nSMase2 being dominant in hypertrophic chondrocytes (Fig. 7*F*). Hyaluronan not only localized to the extracellular matrix of Has2-expressing chondrocytes in immature cartilage but also existed in the matrix of hypertrophic chondrocytes (Fig. 7*F*), suggesting that the low turnover rate may have caused its retention in the cartilage matrix, even after a decrease in Has2. Finally, we checked if the PI3K or Akt pathway was involved in the suppressive action of *Smpd3*/nSMase2 on *Has2*. The accelerated expression of *Has2* by silencing of *Smpd3* in the presence